Shear Stress Regulates Adhesion and Rolling of CD44+ Leukemic and Hematopoietic Progenitor Cells on Hyaluronan

Christof Christophis,[†] Isabel Taubert,[‡] Georg R. Meseck,[†] Mario Schubert,[‡] Michael Grunze,[†§] Anthony D. Ho,[‡] and Axel Rosenhahn[†§*]

[†]Applied Physical Chemistry and [‡]Department of Medicine V, University of Heidelberg, Heidelberg, Germany; and [§]Institute of Functional Interfaces, Karlsruhe Institute of Technology, Karlsruhe, Germany

ABSTRACT Leukemic cells and human hematopoietic progenitor cells expressing CD44 receptors have the ability to attach and roll on hyaluronan. We investigated quantitatively the adhesion behavior of leukemic cell lines and hematopoietic progenitor cells on thin films of the polysaccharides hyaluronan and alginate in a microfluidic system. An applied flow enhances the interaction between CD44-positive cells and hyaluronan if a threshold shear stress of 0.2 dyn/cm^2 is exceeded. At shear stress ~1 dyn/cm^2, the cell rolling speed reaches a maximum of 15 μm/s. Leukemic Jurkat and Kasumi-1 cells lacking CD44-expression showed no adhesion or rolling on the polysaccharides whereas the CD44-expressing leukemic cells KG-1a, HL-60, K-562, and hematopoietic progenitor cells attached and rolled on hyaluronan. Interestingly, the observations of flow-induced cell rolling are related to those found in the recruitment of leukocytes to inflammatory sites and the mechanisms of stem-cell homing into the bone marrow.

INTRODUCTION

Cell adhesion is an important prerequisite for the cell cycle, cytokinesis, and proliferation, and therefore cell survival. The control of the interaction and the response of cells to artificial surfaces is important for implants (1), artificial tissue (2), control of cellular differentiation (3), and for the prevention of biofouling (4). In all mentioned cases, the adhesion of cells to artificial surfaces is critical for the corresponding cellular behavior. One key parameter to characterize the interaction of cells with surfaces is the adhesion strength (5). The ability of a cell to stick to the surface is based on the interaction of adhesion proteins and the extracellular matrix with the surface.

Hyaluronan (hyaluronic acid, HA) is one of the major components found in the extracellular matrix. In addition to its function as cellular material, e.g., in osteoblasts, osteoclasts, stromal, and endothelial cells, HA is important in the regulation of self-renewal, maintenance, and differentiation of hematopoietic progenitor cells (HPC) and leukemic stem cells in the stem cell niche (6,7). The bioactivity of the anionic glycosaminoglycan HA ($pk_a = 3.36$) is based both on physical and chemical properties (8,9). The outstanding rheological properties as a hydrogel designate HA as a structural component in tissue and joints, which is reflected in enrichment in the synovial fluid and the vitreous humor, where it enhances the biomechanical stability (10–12). Interestingly, when HA is applied as coating, it prevents postsurgery adhesion of microorganisms and inflammation as it has been shown in animal studies (1). This resistance against microorganisms was confirmed in studies with cells, bacteria, algae, and barnacle cyprids and depends on the ion strength of the medium (13,14). One reason for the inertness of HA coatings might lie in its hydrogel nature, which involves a high degree of hydration as an important prerequisite for inertness (15,16).

The binding of HA to hyaladherins is involved in many processes like wound healing, inflammation, growth of tumors, and the proliferation of cells (1,17–19). Hyaladherins comprise many proteins capable of binding to HA, but CD44 remains the best-investigated and pivotal binding partner (20–24). CD44 is a multifunctional, ubiquitously expressed transmembrane protein (25–27). The specific binding of CD44 to HA arises from a binding region—the link module—which is common for many hyaladherins (28). It was found that lymphocyte rolling is mediated by CD44 and its binding to HA, which is present on the surface of endothelial cells (29,30) or immobilized on surfaces (31). Additionally, Clark et al. (29) showed that rolling of lymphocytes on tonsillar stroma also depends on the interactions of CD44 and HA.

Inhibition of CD44 with monoclonal antibodies, soluble HA, and hyaluronidase treatment of the substrate reduces adhesion and rolling (29). However, in some cases antibody treatment fails to suppress adhesion, and not all CD44-expressing blood-related cells attach and roll on HA (22,32). Other CD44 functionalities such as posttranslational carbohydrate modifications of CD44 (28,33) and other cell receptors like integrin VLA-4 (34) or the size of the HA binding partner (35) may play a major role in the binding of CD44 to HA. The mechanism of CD44-mediated rolling on HA seems to be complementary to the well-known function of integrins and selectins in lymphocyte homing (36–40).

Still, shear-stress-dependent attachment and detachment as found for selectins in leukocyte adhesion and rolling

Submitted March 16, 2011, and accepted for publication May 23, 2011.

*Correspondence: axel.rosenhahn@kit.edu

Editor: Lewis H. Romer

0006-3495/11/08/0585/9 $2.00

doi: 10.1016/j.bpj.2011.05.045

(41,42) have not yet been reported for CD44/HA interaction. Furthermore, binding of HA to CD44 is involved in the invasion and metastasis in many tumors, such as (for example) in colon carcinoma (43). Moreover, the homing of leukemic stem cells and their engraftment to their niche is CD44-dependent (44). CD44 activation with an antibody inhibited leukemic repopulation in NOD/SCID mice transplanted with human acute myeloid leukemia cells. Related to these findings, Avigdor et al. (45) could show that CD44 and HA are essential for the homing and engraftment of HPCs into the bone marrow and spleen of NOD/SCID mice.

Despite these important findings, there is still a lack of quantitative data to describe the interaction of CD44-positive blood cells with HA under flow. Although rolling of lymphocytes on HA-expressing tonsillar stoma cells has been demonstrated (29), to our knowledge it has not yet been explored whether myeloid leukemia cells and HPCs show rolling on pure HA and it is currently unknown whether the interaction is stimulated by an applied shear stress. Therefore, the interaction of HPCs, CD44+, and CD44− leukemic cell lines to thin films of pure hyaluronan (HA) and alginate (AA) (with the latter used as control for nonspecific adhesion) was studied in detail with a microfluidic setup (15).

MATERIALS AND METHODS

Preparation and characterization of the surfaces

Thin films of polysaccharides on glass slides were prepared following published protocols (46–49). Nexterion B glass slides (Schott, Mainz, Germany) were subjected to an oxygen plasma at 0.5 mbar partial pressure and 150 W for 3 min. Together with a beaker containing 0.6 mL of APTES (3-aminopropyltriethoxysilane), the cleaned and activated substrates were put into a desiccator. After evacuation to 50 mbar, the chemical vapor deposition was carried out in an oven at 150°C within 1 h to form an amino functional surface. The samples were rinsed and ultrasonicated with ethanol (p.a.), blown dry in a stream of nitrogen, and stored under argon until use. HA (molecular mass = $1.63*10^6$ Da) and AA were coupled to the amino functional surfaces by 1-ethyl-3-[3-dimethylaminopropyl]carbodiimide hydrochloride/*n*-hydroxysuccinimide (EDC/NHS) chemistry.

Under vigorous stirring, 1 mg/mL of the respective sodium salt of the polysaccharide (both Sigma-Aldrich, Munich, Germany) was dissolved in 10 mM HEPES buffer. The carboxylic groups in the polysaccharide were subsequently activated by adding NHS (0.05 M) and EDC (0.1 M) under further stirring for 20 min. Coupling to the surface was achieved by immersion of the amino functional glass slides into the activated polysaccharide solution. After 18 h on a shaker table, the reaction was terminated by dilution with 2 L of purified water. Further, the immersion was daily exchanged by purified water for three days to remove uncoupled polysaccharides and EDC/NHS residues. The substrates were blown dry in a stream of nitrogen and stored under argon until use. After each step, the films were characterized by contact angle goniometry, spectral ellipsometry, and x-ray photoelectron spectroscopy using Scofield photoionization cross sections (50).

Cell culture

All work was done under sterile conditions. Five different human leukemic cell lines were used: the acute myeloid leukemia cell lines KG-1a, Kasumi-1, and HL-60; the T cell leukemia Jurkat; and K-562, a chronic myeloid leukemia in blast crisis. Cells were cultured in 75 cm^2 culture flasks in 10 mL RPMI 1640 supplemented with 10% fetal calf serum, 1% penicillin/streptomycin, and 1% L-glutamine. Incubation was carried out in a humidified incubator with 5% CO_2 at 37°C. The cells were split 1 into 5 every 3–4 days. The concentration was set to 10^6 cells/mL before use.

Additionally, CD34+ HPC cells were used. These cells were isolated from human umbilical cord blood after density gradient centrifugation and magnetic cell separation using monoclonal anti-CD34 antibodies conjugated with magnetic microbeads in an AutoMACS system (Miltenyi Biotec, Bergisch-Gladbach, Germany). The purity of the enriched CD34+ HPC subpopulation after magnetic cell separation was checked by flow cytometry using anti-CD34-phycoerythrin (clone 8G12; Becton Dickinson, Heidelberg, Germany) and a FACScan flow cytometry system (Becton Dickinson). A quantity of 98.09% (SD 0.50%) of the cells expressed CD34 on their surface and could therefore be considered as a highly enriched HPC subpopulation.

Adhesion assay

To investigate the adhesion of KG-1a and Jurkat to HA, we modified the adhesion assay of Wagner et al. (51), which based on gravitational force upon inversion. Instead of using human mesenchymal stromal cells, we used the prepared HA slides as an adhesive layer. KG-1a and Jurkat cells were stained with the fluorescent membrane dye PKH26 (Sigma-Aldrich, St. Louis, MO) and then 10,000 cells of each were seeded into a well on the HA slide in cell-culture medium. After an incubation time of three hours, the slide was flipped and incubated for an one additional hour. Adherent cells remained attached to the HA, whereas nonadherent cells dropped down. Images of the adherent and the nonadherent cells were taken using an inverted microscope.

Microfluidic cell detachment assay

Cell-surface interactions can quantitatively be studied by various techniques including spinning disk, micromanipulation, and microfluidics (5). In this work, we used a custom-built microfluidic setup as described in detail in earlier work (15). In brief, the setup comprises an incubator-housed inverted microscope and a parallelized channel system as major components. The channel (25.0 mm × 1.5 mm × 145 μm) is situated between a glass slide and the substrate of interest. The shear stress along the channel walls generated by a liquid flow can be described according to Poiseuille's model (52) with Eq. 1. The wall shear stress τ, referred to as shear stress, depends on the volumetric flow rate Q, the viscosity of the fluid μ (~0.72×10^{-3} kg m^{-1} s^{-1} for cell medium at 37°C (53)), and the channel dimensions of height h and width w. This simple model is in good agreement with three-dimensional numerical calculations (54) and with literature following the Purday approximation (53).

$$\tau = \frac{6Q\mu}{h^2 w} \quad (1)$$

The flow is controlled by a custom-built syringe pump at the channel outlet. For the cell detachment assay, the flow is raised every 5 s by 26% to probe the wall shear stress over five orders of magnitude. That way, the fraction of adherent cells can be determined by time-lapse microscopy and plotted against a logarithmic shear stress scale (15). The critical shear stress τ_{50}, which occurs when 50% of adherent cell population is removed, is assigned to the mean adhesion strength of the cell population (55). The same experimental setup has been used to investigate cell rolling at low shear forces.

Flow cytometry

The cell surface expression of CD44 was investigated by staining the five different leukemic cell lines with anti-CD44-phycoerythrin (clone G44-26; Becton Dickinson) and analyzing them using a FACScan flow cytometry system (Becton Dickinson).

Immunofluorescence microscopy

To investigate the cell surface distribution of CD44 on the five different leukemic cell lines, the cells were first fixated with 2% paraformaldehyde. CD44 was visualized using monoclonal anti-human CD44 clone A3D8 (Sigma-Aldrich) and a secondary anti-mouse Alexa Fluor 488 antibody (Molecular Probes, Leiden, The Netherlands). DNA, as a control for cell viability, was stained with Hoechst 23342 (Roche Diagnostics, Mannheim, Germany). Images were taken with an inverted microscope.

RESULTS

Surface characterization

Activation of the glass supports was achieved by plasma treatment which rendered the surfaces hydrophilic ($\theta < 10°$) (49). Chemical vapor deposition of APTES on the substrates led to an increase in the contact angle ($\theta = 33–42°$) due to the short amino-terminated alkylic chains. Subsequent grafting of the polysaccharides was achieved by EDC/NHS coupling and resulted again in hydrophilic surfaces (AA: $\theta < 10–25°$, HA: $\theta < 10°$), in agreement with literature values (14,49). Spectral ellipsometry gave a thickness of 78.6 Å (SD 23.6 Å) for HA and 21.7 Å (SD 3.9 Å) for AA. Considering the high average molecular mass of the HA used ($M_r = 1.6 \times 10^6$ Da), the polymer is likely to establish multiple connection points, resulting in a rather loose mesh. X-ray photoelectron spectroscopy analysis confirmed the successful coupling in accordance with the comprehensive studies by Stile et al. (49) and our previously published data (14).

KG-1a cells bind specifically to hyaluronan

The interaction of two leukemic cell lines (CD44+ and CD44−) with covalently coupled thin films of AA and HA was investigated. The cell lines of choice were KG-1a cells, which have a high CD44 expression and Jurkat cells, which do not express CD44 (56,57). Parallel experiments on pristine glass were performed to control the viability of the cells and to serve as laboratory standard for comparison.

In the static adhesion assay, based on gravitational force upon inversion (51), we found generally a low adhesion of the leukemic cells to HA. A quantity of 13% of the CD44+ KG-1a cells adhered to HA in comparison to almost no CD44− Jurkat cells (1.6%).

To determine the influence of HA toward cell adhesion quantitatively, we measured the adhesion strength with a microfluidic cell detachment assay (15). KG-1a and Jurkat cells were incubated with supplemented RPMI-1640 medium at 37°C and 5% CO_2 on HA, AA, and pristine glass inside the channels for 3 h. Afterwards, in performing the cell detachment assay, a exponentially increasing flow was applied and the adherent cells were manually counted by analyzing the time-lapse microscopy videos. Statically attached cells and cells which were slowly rolling on the substrate were assigned as adherent ones. Cells which were floating with velocity of the liquid flow (speed of ~25 μm/s per 0.1 dyn/cm^2 shear stress) could easily be distinguished from rolling cells and were considered nonadherent.

Fig. 1 shows the detachment curves for Jurkat and KG-1a on the three substrates. The standard error was calculated from the three to six runs each experiment was conducted. As it can be seen for both cell types, the discrimination of nonadherent from adherent cells appears clearly at a very small shear stress of ~0.05 dyn/cm^2 and results in an initial drop of the cell number. The remaining (adherent) cells require a much higher flow to be removed. Thus, the fraction of initially adherent cells can be calculated as a measure of how readily cells adhere to the surface.

The experiment involving Jurkat cells (Fig. 1 *A*) shows that 56% of the seeded cells adhere to glass while this fraction significantly decreases to 26% on AA and 3% on HA. To quantify the adhesion strength we determined the critical

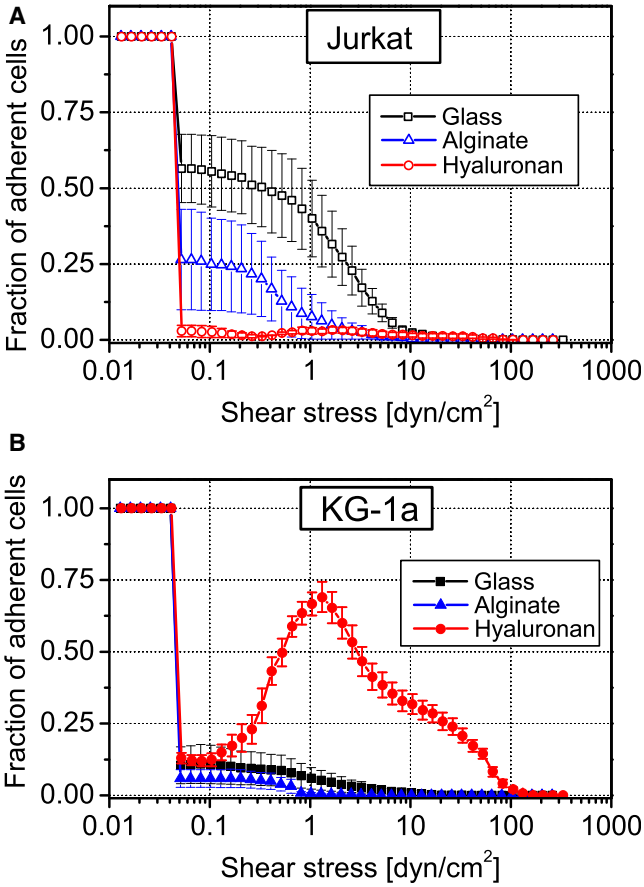

FIGURE 1 Adhesion behavior of leukemic cells on AA and HA. Detachment curves are normalized to initial cell number in the field of view (~600). (*A*) Detachment curves of Jurkat cells on glass (*open squares*), AA (*open triangle*), and HA (*open circles*). (*B*) Detachment curves of KG-1a cells on glass (*solid squares*), AA (*solid triangle*), and HA (*solid circles*). Error bars indicate the mean ± SE. Note that the increase in fraction of adherent cells in panel *B* is due to shear-stress-induced readsorption as discussed in the text.

shear stress (τ_{50}) needed to remove 50% of the adherent cells (15). The values obtained follow the above-determined fraction of adherent cells with the strongest adhesion of 1.48 dyn/cm^2 on glass decreasing to 0.49 dyn/cm^2 on AA and <0.06 dyn/cm^2 on HA (Fig. 2). Thus, the presence of covalently coupled HA or AA on glass does not only render the surfaces less attractive for adhesion but also weakens the adhesion strength of Jurkat cells. These results are in line with the fibroblast studies by Morra and Cassineli (13) and emphasize that polysaccharide coatings are rather inert to cell adhesion if no specific interaction is possible.

The results for the CD44-expressing KG-1a cells are more complicated (Fig. 1 *B*). First of all, KG-1a cells show a generally reduced tendency to adhere to glass compared to Jurkat, as only 10% of the seeded cells adhere. On AA substrate, the adhesion is further reduced to a fraction of only 6%. In contrast to that, the HA substrate shows, with 13% adherent fraction of KG-1a cells, an increase—even with respect to glass. A puzzling result which we so far never observed in our microfluidic experiments (e.g., for Jurkat) is the increase in number of cells on the surface with increasing shear stress >0.2 dyn/cm^2.

At this point, we have to note an important experimental detail: Though pure medium was used during the detachment assay to flush the channel, especially in the beginning, there are residual cells located in the tubing and the part of the channel upstream from the observed field of view. These cells are flushed into the field of view and seem to attach more readily than during 3 h of static incubation. Thus, the flow seems to stimulate KG-1a cells to bind to HA, leading to a temporary increase of the cell number during the experiment. At higher shear stress, cells are removed and the τ_{50} diminishes from 1.40 dyn/cm^2 on glass to 0.56 dyn/cm^2 on AA and reaches a maximum of 5.17 dyn/cm^2 on HA (Fig. 2). Both the adhesion strength and the fraction of adherent KG-1a cells are enhanced with HA present on the surface.

Flow activates the binding of KG-1a to hyaluronan

The above observation of flow-induced adhesion was possible because cells still present in the tubing upstream of the observation area were rinsed into the channel. However, supply of cells in this experiment was not controlled and thus we designed a more systematic experiment. KG-1a cells (~600) were seeded inside the microfluidic channel for 5 min to allow sinking down to the surface by gravity and to establish a physical contact to the surface. Subsequently, a constant flow was applied to stimulate adhesion of the resting cells. The experiment was conducted for each shear stress three times. After 10 s of shear stress the fraction of adherent, i.e., the fraction of nonfloating cells, was determined for a series of different shear stresses (Fig. 3). The maximum number of adherent cells was found at a shear stress of 1.0 dyn/cm^2. This value is only slightly below the 1.3 dyn/cm^2 derived from the dynamic cell detachment experiment described above (*dotted curve* reproduced from Fig. 1 *B*).

Additionally to the number of adherent cells, their rolling speed in dependence of applied shear stress was analyzed. As pointed out above, rolling cells can easily be distinguished from cells passively driven by the liquid flow due to their strongly decreased velocity (2 μm/s vs. 25 μm/s at 0.1 dyn/cm^2). We recorded movies of rolling cells by microscopy and cells ($n > 30$) were tracked during 60 s of constant flow to calculate their rolling speed (Fig. 4). We note a linear increase in velocity from ~2.0 μm/s to ~11.5 μm/s when the shear stress is increased from

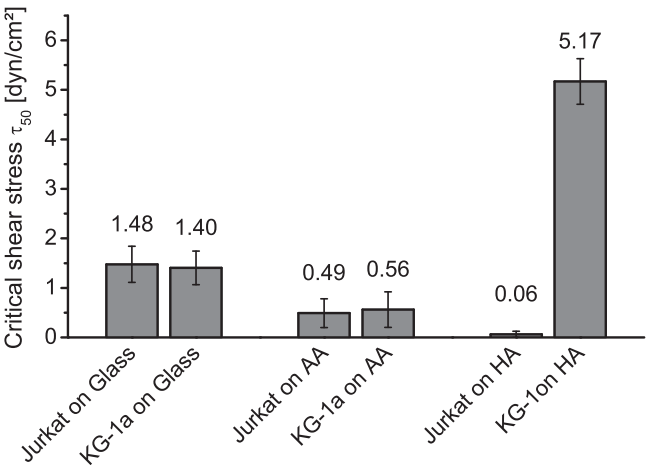

FIGURE 2 Critical shear stress as a measure of cell adhesion strength of Jurkat and KG-1a cell lines on glass, AA, and HA. Cell adhesion strength is approximately the same for both cell lines on glass and AA but not on HA. Error bars represent standard error.

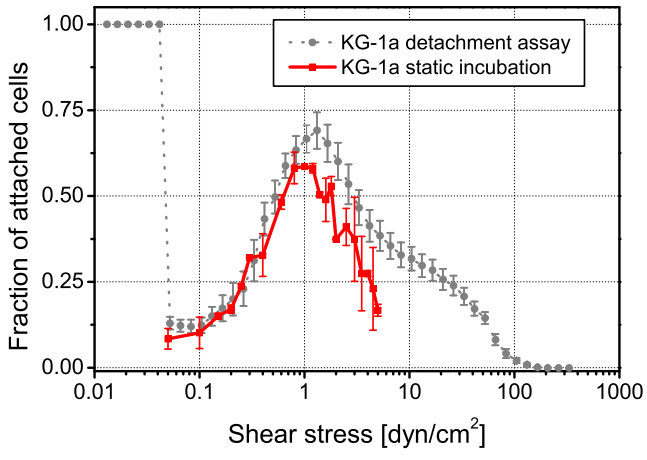

FIGURE 3 Comparison of KG-1a on HA flow activation measured by two different assays. Curves as determined by the cell detachment assay (same data as in Fig. 1 *B*, *solid circles*) and the constant flow assay (*solid squares*). The maximum for both experiments is ~1 dyn/cm^2. Error bars represent standard error.

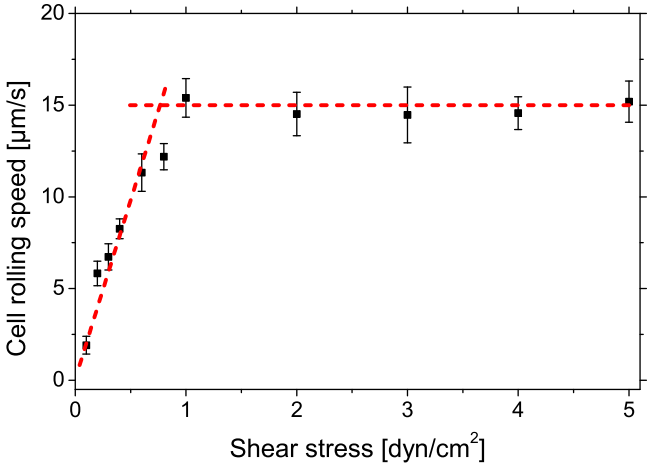

FIGURE 4 Cell rolling speed in dependence upon applied shear stress. Rolling speed increases linearly up to 0.6 dyn/cm^2. Maximum cell rolling speed is reached at ~1 dyn/cm^2. (*Solid squares*) Measured data. (*Dotted lines*) Linear increase and the saturation rolling speed. Error bars show standard error.

0.1 dyn/cm^2 to 0.6 dyn/cm^2. At higher shear stress, the cells reach a maximum rolling speed of ~15 μm/s, which remains constant even at further increasing flow rates. The transition between the linear increase and the fixed rolling speed occurs at ~1 dyn/cm^2. This supports the findings of the adhesion experiments, which showed an enhanced interaction of KG-1a cells and the HA-coated surface for shear flows of ~1 dyn/cm^2.

CD44 expression is a prerequisite for shear-stress-induced binding to hyaluronan

We further tested the concept of flow-induced binding toward five leukemic cell lines with different CD44 expression on HA. CD44 expression and distribution on the surface was determined by flow cytometry and immunofluorescence microscopy (Fig. 5). Jurkat and Kasumi-1 cells showed no CD44 expression. K-562 cells showed a very heterogeneous expression. Cells with a high and a medium expression, but also cells without any CD44 expression, were detected. KG-1a and HL-60 cells had a very high CD44 expression.

To compare the flow activation of the different cells to HA-coated surfaces, we used a constant flow assay and analyzed the flow-induced accumulation of cells. As evident from the flow cytometry measurements, some of the cells had only low CD44-expression. Thus, a comparably low shear stress of 0.2 dyn/cm^2 was chosen to just stimulate flow-activated adhesion but not to remove weakly adherent cells. The constant flow assay was performed nine times. We found that all CD44-expressing cell lines attach from flow on HA whereas none of the two CD44− cell lines attach (Fig. 6). Cell attachment for HL-60 is highest after 4 min (~810 cells, ~100% CD44) followed by KG-1a (~340 cells, ~100% CD44) and K-562 (~190 cells, ~92% CD44).

Although the relative trend that CD44 expression enhances the sticking ability on HA is obvious, it is not possible to find a linear correlation between CD44 expression and attachment rate, as, e.g., HL-60 and KG-1a show similar expression but different attachment probability. One reason

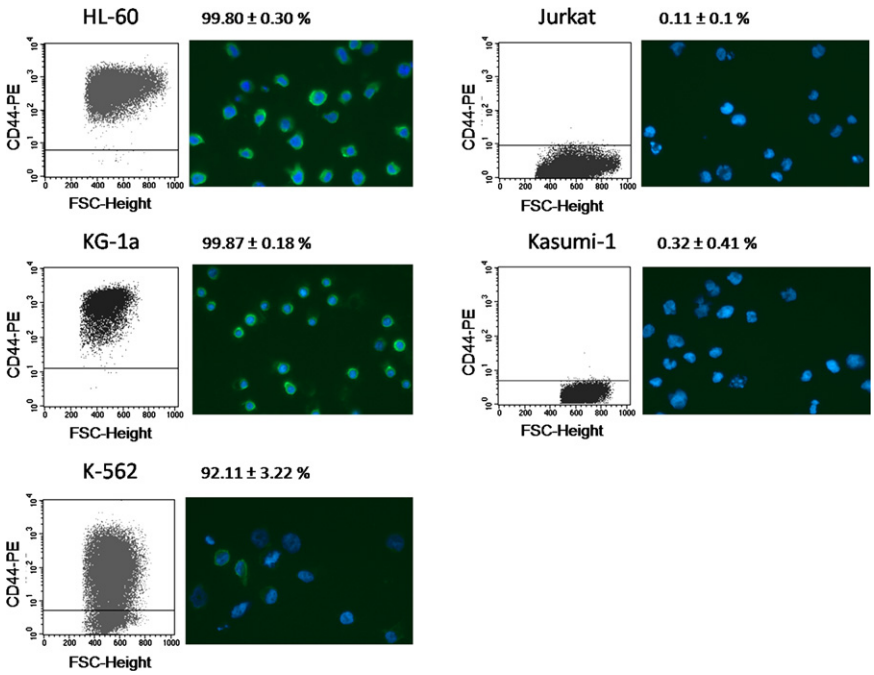

FIGURE 5 Flow cytometry and immunofluorescence microscopy images of CD44 on the five leukemic cell lines used in the microfluidic flow incubation assay. For flow cytometry, anti-CD44$^-$ PE (*clone G44-26*) was used. Percentages for the mean ± SD of CD44+ cells of at least three experiments are shown. For immunofluorescence microscopy, DNA was stained with Hoechst 23342 (*blue*) and CD44 with the clone A3D8 and Alexa Fluor 488 (*green*).

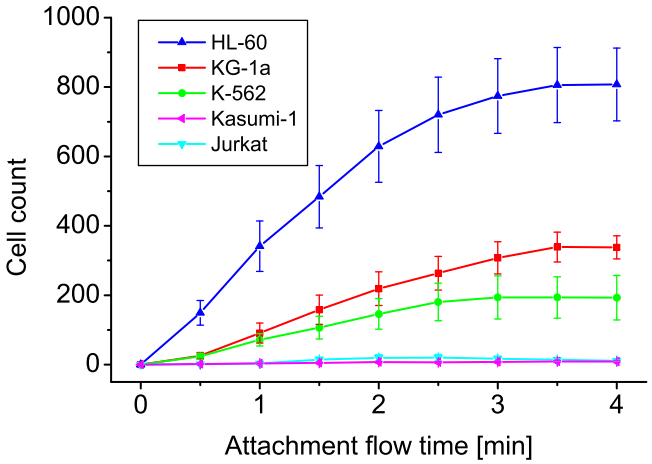

FIGURE 6 Constant flow assay for leukemic cell lines expressing different amounts of CD44. The applied shear stress during incubation was ~0.2 dyn/cm^2. Cell attachment occurs only for CD44+ cell lines. Error bars represent the standard error.

could be the different cell size (HL-60: 14.86 μm, SD 2.51 μm and KG-1a (12.97 μm, SD 1.63 μm)), as larger cells rolling on the surface are exposed to a higher shear stress because they physically extend further into the parabolic flow profile. Theoretical predictions based on geometric considerations reveal that the hydrodynamic force acting on the cell increases with the square of the radius (58). This could lead to an enhanced flow activation of HL-60 compared to KG-1a at the same applied wall shear stress, and therefore a higher attachment rate. Also, cell-line specific regulation and expression of further receptors (e.g., VLA-4) are involved in the adhesion process to HA (34).

Hematopoietic progenitor cells bind specifically to hyaluronan

To show that the findings above on leukemic cell lines have relevance for isolated human primary material, the impact of HA interactions toward clinical relevant hematopoietic stem cells was clarified. Therefore, HPCs, enriched from umbilical cord blood, were incubated on HA and AA substrates inside the channel system as described in the last section. HPCs have a high CD44-expression (mean 98.78%, SD 0.81%). Unfortunately, access to this isolated human material is limited and it was impossible to repeat the full experimental series conducted for the leukemic cell lines. Thus, we restricted these experiments to single cells in the microfluidic channel and a phenomenological description of the observations when a shear flow is applied.

Conducting the cell detachment assay two times revealed that HPCs do not adhere on AA (0%) and only a few adhere on HA (6%). Still, upon raising shear stress, more HPCs adhere and roll in dependence upon the shear stress (velocity of ~14 μm/s at 0.5 dyn/cm^2 and ~18 μm/s at 1.0 dyn/cm^2) on HA and detach at relatively high shear stress of 2.17 dyn/cm^2, similar to the case of KG-1a. The limited number of cells in this experiment (~100) does not allow a more elaborate analysis, but we could support this observation by a descriptive experiment: When keeping the shear stress constant at 2 dyn/cm^2 and switching the liquid flow direction, the HPCs follow the flow direction instantly while keeping contact with the surface at a velocity of 17.8 μm/s (Fig. 7, and see Movie S1 in the Supporting Material).

As it is described for catch-bond activation (58), Movie S1 and Movie S2 show that rolling cell adhesion of HPCs is characterized by consecutive moving and attachment phases. Whenever the flow is switched off and the liquid flow slowly decays, first HPCs arrest at 0.3 dyn/cm^2 on HA then retract the filopodia contacts at ~0.2 dyn/cm^2 and detach from the surface (Fig. 8, and see Movie S2). The fact that the surface contact is lifted becomes visible in the velocity, which is much higher than for the rolling cells at higher flow velocities. Thus, HPCs also have a strong interaction with HA, as visible in adhesion strength and the tendency to roll at the surface. The shear force induction is also visible, as cells which are not exposed to the shear force for a certain time lift their surface contact and go with the flow. Thus, the descriptive observations on HPCs

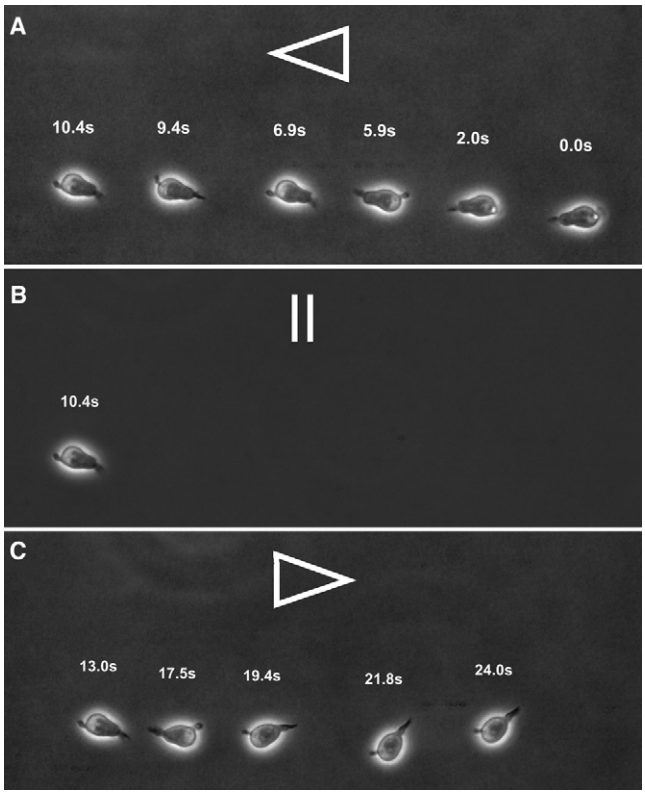

FIGURE 7 Image sequence of a rolling HPC cell on HA inside a microfluidic channel. (*Arrows*) Flow direction. The mean rolling speed is 17.8 μm/s at a liquid flow corresponding to a shear stress of 2 dyn/cm^2 in the same direction (*A* and *C*). The cell rolling direction changes instantly when the flow direction is switched (*B*).

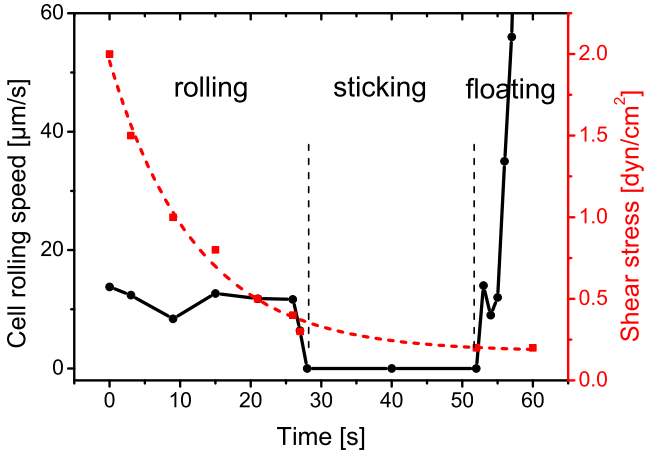

FIGURE 8 Cell rolling speed of a single HPC in dependence upon applied shear stress. At shear stress below 0.3 dyn/cm^2 (*dotted curve*), the HPC is in the arrest state (*solid curve*). HPC retracts filopodia and detaches from the surface when shear stress decreases to 0.2 dyn/cm^2.

isolated from human cord blood show that the concept of flow-activated adhesion also occurs in medically relevant material.

DISCUSSION

In this study, we investigated the specific interaction between hyaluronan and leukemic cell lines and umbilical cord blood hematopoietic progenitor cells (HPCs). Studies by Morra and Cassineli (13) previously showed the general inertness of hydrogel-like polysaccharide coatings, which is most likely due to their strong hydration. The latter might present an important prerequisite to prevent adhesion (15,16). Our study confirms the inertness of such coatings and a low adhesion strength is observed for Jurkat on AA (τ_{50} = 0.49 dyn/cm^2), on HA (τ_{50} = 0.06 dyn/cm^2), and for KG-1a on AA (τ_{50} = 0.56 dyn/cm^2). For CD44+ KG-1a on HA, a stronger adhesion is observed (τ_{50} = 5.17 dyn/cm^2).

The accumulation of KG-1a on HA during the shear force assay for shear stresses at or higher 0.2 dyn/cm^2 indicates that the interaction is shear-stress-mediated, so cell adhesion and rolling on HA are stimulated by the presence of a shear force. Interestingly, the values directly correspond to the ones found for selectin-dependent leukocyte rolling (41,42). Experiments using constant flow conditions reveal that the fraction of adherent cells and the rolling speed of KG-1a cells on HA depend nonlinearly on the shear stress present. The maximum adhesion fraction and thus the highest cellular response were found at ~1 dyn/cm^2. In agreement with these findings, the cell rolling speed correlates linearly with shear stress at low ranges but becomes saturated above 1 dyn/cm^2. This observation is in line with previous findings by Finger et al. (41) and Zhu et al. (59) for the selectin-dependent leukocyte rolling.

From our observations, we can conclude the following mechanism: KG-1a cells respond to a flow and attach to the HA substrate. The cells roll on HA with a specific speed that is proportional to the applied shear stress. Beyond a certain flow, cell binding to HA is activated and the cells actively resist further acceleration by the enhanced surface interaction. At even larger shear stress, the Stokes force on the cells exceeds the binding strength to the surface and the cells are removed. The mechanism of bond strengthening remains unclear, but one might speculate on catch bond theory (60) or additional other transport mechanisms (59) known from leukocyte rolling. CD44+ KG1a, HL-60, and K-562 cells show a much higher attachment compared to CD44− Jurkat and Kasumi-1 cells. The results indicate that CD44 expression is a prerequisite for adhesion to HA (31), and (to our knowledge) it was for the first time observed that CD44+ leukemia cells roll on pure HA surfaces. As reported by Lesley et al. (31), lymphocytes show a similar behavior, because rolling on synthetic HA requires the presence of CD44.

Unfortunately, the mechanism behind CD44-dependent binding to HA is still controversial and not yet fully understood (61), as not all CD44-expressing blood-related cells attach to HA (22,32). Further experiments to unravel the specific role of different adhesion receptors are anticipated for the future but exceed the scope of the work here, which is focused on the shear-stress regulated adhesion. Up to now it was unknown, to our knowledge, whether the interaction of leukemia cells with HA is stimulated by flow. We found that a minimum external shear stress (0.2 dyn/cm^2) strongly enhances the interaction of CD44+ cells with hyaluronan (flow-induced rolling and adhesion). The clinical relevance was demonstrated by the flow-induced interaction between HPCs that were isolated from cord blood; thus, the observations in cell lines were unequivocally validated.

To our knowledge, this is the first time that rolling and flow-induced and regulated adhesion of hematopoietic progenitor cells on hyaluronans was observed. These results indicate that flow-mediated adhesion is an important concept valid beyond lymphocyte rolling on endothelial cells (29,30) or immobilized HA (31). The shear-stress-regulated adhesion on HA is especially interesting because the CD44/HA interaction plays an important role for homing and engraftment of HPCs into the bone marrow which has been shown in spleen of NOD/SCID mice (45). It is possible that the mechanism of HPC and leukemic cell adhesion on HA might be similar to the one discussed for selectin-based leukocyte rolling in inflammatory response, and thus the shear-stress-regulated adhesion represents a more general principle than so far anticipated.

SUPPORTING MATERIAL

Two movies are available at http://www.biophysj.org/biophysj/supplemental/S0006-3495(11)00646-1.

We thank Dr. Rainer Saffrich for the help with the immunofluorescence microscopy.

A part of this work was supported by Office of Naval Research grant No. N00014-08-1-1116, the Sander Stiftung (grant No. 2010.079.1), the POF program Biointerfaces of the Helmholtz Gemeinschaft, and by the Nationale Centrum für Tumorerkrankungen Heidelberg.

REFERENCES

1. Morra, M. 2005. Engineering of biomaterials surfaces by hyaluronan. *Biomacromolecules.* 6:1205–1223.
2. Khademhosseini, A., R. Langer, …, J. P. Vacanti. 2006. Microscale technologies for tissue engineering and biology. *Proc. Natl. Acad. Sci. USA.* 103:2480–2487.
3. McBeath, R., D. M. Pirone, …, C. S. Chen. 2004. Cell shape, cytoskeletal tension, and RhoA regulate stem cell lineage commitment. *Dev. Cell.* 6:483–495.
4. Rosenhahn, A., T. Ederth, and M. E. Pettitt. 2008. Advanced nanostructures for the control of biofouling: the FP6 EU Integrated Project AMBIO. *Biointerphases.* 3:IR1–IR5.
5. Christ, K. V., and K. T. Turner. 2010. Methods to measure the strength of cell adhesion to substrates. *J. Adhes. Sci. Technol.* 24:2027–2058.
6. Calvi, L. M., G. B. Adams, …, D. T. Scadden. 2003. Osteoblastic cells regulate the hematopoietic stem cell niche. *Nature.* 425:841–846.
7. Wilson, A., and A. Trumpp. 2006. Bone-marrow hematopoietic-stem-cell niches. *Nat. Rev. Immunol.* 6:93–106.
8. Fraser, J. R. E., T. C. Laurent, and U. B. G. Laurent. 1997. Hyaluronan: its nature, distribution, functions and turnover. *J. Intern. Med.* 242: 27–33.
9. Park, J. W., and B. Chakrabarti. 1978. Optical characteristics of carboxyl group in relation to the circular dichroic properties and dissociation constants of glycosaminoglycans. *Biochim. Biophys. Acta. General Subjects.* 544:667–675.
10. Meyer, K., and J. Palmer. 1934. The polysaccharide of the vitreous humor. *Biol. Chem.* 107:629–634.
11. Comper, W. D., and T. C. Laurent. 1978. Physiological function of connective tissue polysaccharides. *Physiol. Rev.* 58:255–315.
12. Chen, W. Y. J., and G. Abatangelo. 1999. Function of hyaluronan in wound repair. *Wound. Rep. Reg.* 7:79–89.
13. Morra, M., and C. Cassineli. 1999. Non-fouling properties of polysaccharide-coated surfaces. *J. Biomater. Sci. Polym. Ed.* 10:1107–1124.
14. Cao, X. Y., M. E. Pettit, …, A. Rosenhahn. 2009. Resistance of polysaccharide coatings to proteins, hematopoietic cells, and marine organisms. *Biomacromolecules.* 10:907–915.
15. Christophis, C., M. Grunze, and A. Rosenhahn. 2010. Quantification of the adhesion strength of fibroblast cells on ethylene glycol terminated self-assembled monolayers by a microfluidic shear force assay. *Phys. Chem. Chem. Phys.* 12:4498–4504.
16. Rosenhahn, A., S. Schilp, …, M. Grunze. 2010. The role of "inert" surface chemistry in marine biofouling prevention. *Phys. Chem. Chem. Phys.* 12:4275–4286.
17. Jiang, D., J. Liang, and P. W. Noble. 2007. Hyaluronan in tissue injury and repair. *Annu. Rev. Cell Dev. Biol.* 23:435–461.
18. Pessac, B., and V. Defendi. 1972. Cell aggregation: role of acid mucopolysaccharides. *Science.* 175:898–900.
19. Evanko, S. P., J. C. Angello, and T. N. Wight. 1999. Formation of hyaluronan- and versican-rich pericellular matrix is required for proliferation and migration of vascular smooth muscle cells. *Arterioscler. Thromb. Vasc. Biol.* 19:1004–1013.
20. Aruffo, A., I. Stamenkovic, …, B. Seed. 1990. CD44 is the principal cell surface receptor for hyaluronate. *Cell.* 61:1303–1313.
21. Isacke, C. M., and H. Yarwood. 2002. The hyaluronan receptor, CD44. *Int. J. Biochem. Cell Biol.* 34:718–721.
22. Lesley, J., R. Hyman, and P. W. Kincade. 1993. CD44 and its interaction with extracellular matrix. *Adv. Immunol.* 54:271–335.
23. Bajorath, J., B. Greenfield, …, A. Aruffo. 1998. Identification of CD44 residues important for hyaluronan binding and delineation of the binding site. *J. Biol. Chem.* 273:338–343.
24. Lesley, J., N. English, …, R. Hyman. 2002. Hyaluronan Binding by Cell Surface CD44. Woodhead Publishing, Cambridge, UK.
25. Ghaffari, S., F. Smadja-Joffe, …, C. Eaves. 1999. CD44 isoforms in normal and leukemic hematopoiesis. *Exp. Hematol.* 27:978–993.
26. Goodison, S., V. Urquidi, and D. Tarin. 1999. CD44 cell adhesion molecules. *MP, Mol. Pathol.* 52:189–196.
27. Marhaba, R., and M. Zöller. 2004. CD44 in cancer progression: adhesion, migration and growth regulation. *J. Mol. Histol.* 35:211–231.
28. Ponta, H., L. Sherman, and P. A. Herrlich. 2003. CD44: from adhesion molecules to signaling regulators. *Nat. Rev. Mol. Cell Biol.* 4:33–45.
29. Clark, R. A., R. Alon, and T. A. Springer. 1996. CD44 and hyaluronan-dependent rolling interactions of lymphocytes on tonsillar stroma. *J. Cell Biol.* 134:1075–1087.
30. DeGrendele, H. C., P. Estess, …, M. H. Siegelman. 1996. CD44 and its ligand hyaluronate mediate rolling under physiologic flow: a novel lymphocyte-endothelial cell primary adhesion pathway. *J. Exp. Med.* 183:1119–1130.
31. Lesley, J., I. Gál, …, K. Mikecz. 2004. TSG-6 modulates the interaction between hyaluronan and cell surface CD44. *J. Biol. Chem.* 279:25745–25754.
32. Hyman, R., J. Lesley, and R. Schulte. 1991. Somatic cell mutants distinguish CD44 expression and hyaluronic acid binding. *Immunogenetics.* 33:392–395.
33. Lesley, J., R. Hyman, …, G. A. Turner. 1997. CD44 in inflammation and metastasis. *Glycoconj. J.* 14:611–622.
34. Nandi, A., P. Estess, and M. Siegelman. 2004. Bimolecular complex between rolling and firm adhesion receptors required for cell arrest; CD44 association with VLA-4 in T cell extravasation. *Immunity.* 20:455–465.
35. Wolny, P. M., S. Banerji, …, R. P. Richter. 2010. Analysis of CD44-hyaluronan interactions in an artificial membrane system: insights into the distinct binding properties of high and low molecular weight hyaluronan. *J. Biol. Chem.* 285:30170–30180.
36. Siegelman, M. H., H. C. DeGrendele, and P. Estess. 1999. Activation and interaction of CD44 and hyaluronan in immunological systems. *J. Leukoc. Biol.* 66:315–321.
37. Milinkovic, M., J. H. Antin, …, R. Sackstein. 2004. CD44-hyaluronic acid interactions mediate shear-resistant binding of lymphocytes to dermal endothelium in acute cutaneous GVHD. *Blood.* 103:740–742.
38. Lawrence, M. B., and T. A. Springer. 1991. Leukocytes roll on a selectin at physiologic flow rates: distinction from and prerequisite for adhesion through integrins. *Cell.* 65:859–873.
39. Ley, K., C. Laudanna, …, S. Nourshargh. 2007. Getting to the site of inflammation: the leukocyte adhesion cascade updated. *Nat. Rev. Immunol.* 7:678–689.
40. Orsello, C. E., D. A. Lauffenburger, and D. A. Hammer. 2001. Molecular properties in cell adhesion: a physical and engineering perspective. *Trends Biotechnol.* 19:310–316.
41. Finger, E. B., K. D. Puri, …, T. A. Springer. 1996. Adhesion through L-selectin requires a threshold hydrodynamic shear. *Nature.* 379:266–269.
42. Lawrence, M. B., G. S. Kansas, …, K. Ley. 1997. Threshold levels of fluid shear promote leukocyte adhesion through selectins (CD62L,P,E). *J. Cell Biol.* 136:717–727.
43. Kim, H. R., M. A. Wheeler, …, K. M. Bullard. 2004. Hyaluronan facilitates invasion of colon carcinoma cells in vitro via interaction with CD44. *Cancer Res.* 64:4569–4576.
44. Jin, L., K. J. Hope, …, J. E. Dick. 2006. Targeting of CD44 eradicates human acute myeloid leukemic stem cells. *Nat. Med.* 12:1167–1174.

45. Avigdor, A., P. Goichberg, …, T. Lapidot. 2004. CD44 and hyaluronic acid cooperate with SDF-1 in the trafficking of human CD34+ stem/progenitor cells to bone marrow. *Blood.* 103:2981–2989.

46. Albersdorfer, A., and E. Sackmann. 1999. Swelling behavior and viscoelasticity ultrathin grafted hyaluronic acid films. *Eur. Phys. J. B.* 10:663–672.

47. Wang, W., and M. W. Vaughn. 2008. Morphology and amine accessibility of (3-aminopropyl) triethoxysilane films on glass surfaces. *Scanning.* 30:65–77.

48. Grabarek, Z., and J. Gergely. 1990. Zero-length crosslinking procedure with the use of active esters. *Anal. Biochem.* 185:131–135.

49. Stile, R. A., T. A. Barber, …, K. E. Healy. 2002. Sequential robust design methodology and x-ray photoelectron spectroscopy to analyze the grafting of hyaluronic acid to glass substrates. *J. Biomed. Mater. Res.* 61:391–398.

50. Scofield, J. H. 1976. Hartree-Slater subshell photoionization cross-sections at 1254 and 1487 eV. *J. Electron Spectrosc. Relat. Phenom.* 8:129–137.

51. Wagner, W., F. Wein, …, A. D. Ho. 2007. Adhesion of hematopoietic progenitor cells to human mesenchymal stem cells as a model for cell-cell interaction. *Exp. Hematol.* 35:314–325.

52. Deen, W. M. 1998. Analysis of Transport Phenomena. Oxford University Press, New York.

53. Young, E. W. K., A. R. Wheeler, and C. A. Simmons. 2007. Matrix-dependent adhesion of vascular and valvular endothelial cells in microfluidic channels. *Lab Chip.* 7:1759–1766.

54. Lu, H., L. Y. Koo, …, K. F. Jensen. 2004. Microfluidic shear devices for quantitative analysis of cell adhesion. *Anal. Chem.* 76:5257–5264.

55. García, A. J., P. Ducheyne, and D. Boettiger. 1997. Quantification of cell adhesion using a spinning disc device and application to surface-reactive materials. *Biomaterials.* 18:1091–1098.

56. Koeffler, H. P., R. Billing, …, D. W. Golde. 1980. An undifferentiated variant derived from the human acute myelogenous leukemia cell line (KG-1). *Blood.* 56:265–273.

57. Schneider, U., H.-U. Schwenk, and G. Bornkamm. 1977. Characterization of EBV-genome negative "null" and "T" cell lines derived from children with acute lymphoblastic leukemia and leukemic transformed non-Hodgkin lymphoma. *Int. J. Cancer.* 19:621–626.

58. Yago, T., J. H. Wu, …, R. P. McEver. 2004. Catch bonds govern adhesion through L-selectin at threshold shear. *J. Cell Biol.* 166:913–923.

59. Zhu, C., T. Yago, …, R. P. McEver. 2008. Mechanisms for flow-enhanced cell adhesion. *Ann. Biomed. Eng.* 36:604–621.

60. Marshall, B. T., M. Long, …, C. Zhu. 2003. Direct observation of catch bonds involving cell-adhesion molecules. *Nature.* 423:190–193.

61. Jackson, D. G. 2009. Immunological functions of hyaluronan and its receptors in the lymphatics. *Immunol. Rev.* 230:216–231.